

## Subregion Action and Complexity

Mohsen Alishahiha<sup>\*</sup>, Komeil Babaei Velni<sup>†</sup> and M. Reza Mohammadi Mozaffar<sup>†,\*</sup>

<sup>\*</sup> *School of Physics, Institute for Research in Fundamental Sciences (IPM)  
P.O. Box 19395-5531, Tehran, Iran*

<sup>†</sup> *Department of Physics, University of Guilan, P.O. Box 41335-1914, Rasht, Iran*

E-mails: [alishah@ipm.ir](mailto:alishah@ipm.ir), [babaeivelni@guilan.ac.ir](mailto:babaeivelni@guilan.ac.ir), [mmohammadi@guilan.ac.ir](mailto:mmohammadi@guilan.ac.ir)

### Abstract

We evaluate finite part of the on-shell action for black brane solutions of Einstein gravity on different subregions of spacetime enclosed by null boundaries. These subregions include the intersection of WDW patch with past/future interior and left/right exterior for a two sided black brane. Identifying the on-shell action on the exterior regions with subregion complexity one finds that it obeys subadditivity condition. This gives an insight to define a new quantity named mutual complexity. We will also consider certain subregion that is a part of spacetime which could be causally connected to an operator localized behind/outside the horizon. Taking into account all terms needed to have a diffeomorphism invariant action with a well-defined variational principle, one observes that the main contribution that results to a nontrivial behavior of the on-shell action comes from joint points where two lightlike boundaries (including horizon) intersect. A spacelike boundary gives rise to a linear time growth, while we have a classical contribution due to a timelike boundary that is given by the free energy.

# Contents

<b>1</b>	<b>Introduction</b>	<b>1</b>
<b>2</b>	<b>Complexity and Subregions Behind the Horizon</b>	<b>4</b>
2.1	CA Proposal . . . . .	4
2.2	Past Patch . . . . .	7
2.3	Intersection of WDW Patch with Past and Future Interiors . . . . .	8
2.3.1	Past Interior . . . . .	9
2.3.2	Future Interior . . . . .	11
2.4	Late Time Behavior . . . . .	12
2.5	Holographic Uncomplexity . . . . .	13
<b>3</b>	<b>Subregion Complexity and Outside the Horizon</b>	<b>15</b>
3.1	Complexity of Layered Stretched Horizon . . . . .	15
3.2	CA Proposal and Subregion Complexity . . . . .	18
<b>4</b>	<b>Discussions and Conclusions</b>	<b>20</b>

---

## 1 Introduction

Based on earlier works of [1, 2] it was conjectured that computational complexity associated with a boundary state may be identified with the on-shell action evaluated on a certain subregion of the bulk spacetime [3, 4]. The corresponding subregion is Wheeler-DeWitt (WDW) patch of the spacetime that is the domain of dependence of any Cauchy surface in the bulk whose intersection with the asymptotic boundary is the time slice on which the state is defined.

This proposal, known as “complexity equals action” (CA), has been used to explore several properties of computational complexity for those field theories that have gravitational dual<sup>1</sup>. In particular the growth rate of complexity has been studied for an eternal black hole in [18]. It was shown that although in the late time the growth rate approaches a constant value that is twice of the mass of the black hole, the constant is approached from above, violating the Lloyd’s bound [19]. Of course this is not the case for a state followed by a global quench [20]. It is worth to mention that recently there has been some progress for studying the computational complexity of a state in field theory [21–32].

So far the main concern in the literature was the growth rate of complexity and therefore the on-shell action was computed up to time independent terms [33–35]. Moreover it was also shown that the time dependent effects are controlled by the regions behind the horizon. We note, however, that in order to understand holographic complexity better it is crucial to have the full expression of it. It is also important to evaluate the contribution of different parts (inside and outside of the

---

<sup>1</sup>We would like to stress that on the gravity side there is another proposal for computing the computational complexity, known as “complexity equals volume” (CV) [1, 2]. The generalization of CV proposal to subsystems has been done in [5] (see also [6–13]). Yet another approach to complexity based on Euclidean path-integral has been introduced in [14–16]. For a recent development and its possible relation with CA approach see [17].

horizon) of the WDW patch, specialty. It is also illustrative to compute on-shell action on a given subregion of spacetime enclosed by null boundaries, that is not necessarily the WDW patch. Indeed this is one of the aim of the present work to carry out these computations explicitly. Moreover we will carefully identify the contribution of each term in the action.

Since we are interested in the on-shell action, it is crucial to make clear what one means by “on-shell action”. In general an action could have several terms that might be important due to certain physical reason. In particular in order to have a well-defined variational principle with Dirichlet boundary condition one needs to add certain Gibbons-Hawking-York boundary terms at spacelike and timelike boundaries [36, 37]. Moreover to accommodate null boundaries it is also crucial to add the corresponding boundary terms on the null boundaries as well as certain joint action at points where a null boundary intersects to other boundaries [38, 39].

Restricted to Einstein gravity and assuming to have a well-defined variational principle one arrives at the following action [39]

$$I^{(0)} = \frac{1}{16\pi G_N} \int d^{d+2}x \sqrt{-g} (R - 2\Lambda) + \frac{1}{8\pi G_N} \int_{\Sigma_t^{d+1}} K_t d\Sigma_t \\ \pm \frac{1}{8\pi G_N} \int_{\Sigma_s^{d+1}} K_s d\Sigma_s \pm \frac{1}{8\pi G_N} \int_{\Sigma_n^{d+1}} K_n dS d\lambda \pm \frac{1}{8\pi G_N} \int_{J^d} a dS. \quad (1.1)$$

Here the timelike, spacelike, and null boundaries and also joint points are denoted by  $\Sigma_t^{d+1}$ ,  $\Sigma_s^{d+1}$ ,  $\Sigma_n^{d+1}$  and  $J^d$ , respectively. The extrinsic curvature of the corresponding boundaries are given by  $K_t$ ,  $K_s$  and  $K_n$ . The function  $a$  at the intersection of the boundaries is given by the logarithm of the inner product of the corresponding normal vectors and  $\lambda$  is the null coordinate defined on the null segments. The sign of different terms depends on the relative position of the boundaries and the bulk region of interest (see [39] for more details).

As far as the variational principle is concerned the above action defines a consistent theory. Nonetheless one still has possibilities to add certain boundary terms that do not alter the boundary condition, but could have nontrivial contribution to the on-shell action. Therefore it is important to fix these terms using certain physical principles before computing the on-shell action.

In particular one can see that the above action is not invariant under a reparametrization of the null generators. Therefore one may conclude that the above action does not really define a consistent theory. Actually to maintain the invariance under a reparametrization of the null generators one needs to add an extra term to the action as follows [39] (see also [40])<sup>2</sup>

$$I^{\text{amb}} = \frac{1}{8\pi G_N} \int_{\Sigma_n^{d+1}} d^d x d\lambda \sqrt{\gamma} \Theta \log \frac{|\tilde{L}\Theta|}{d}, \quad (1.2)$$

where  $\tilde{L}$  is an undetermined length scale and  $\gamma$  is the determinant of the induced metric on the

---

<sup>2</sup> The importance of this term has also been emphasized in [41–43] where it was shown that it is essential to consider the contribution of this term to the complexity.

joint point where two null segments intersect, and

$$\Theta = \frac{1}{\sqrt{\gamma}} \frac{\partial \sqrt{\gamma}}{\partial \lambda}. \quad (1.3)$$

Although even with this extra term the length scale  $\tilde{L}$  remains undetermined, adding this term to action (1.1) would define a consistent theory. Therefore in what follows by evaluating “on-shell action” we mean to consider  $I = I^{(0)} + I^{\text{amb}}$ . We note, however, that the resultant on-shell action may or may not be UV finite. Thus, one may want to get finite on-shell action (as we do for gravitational free energy) that requires to add certain counterterms. Actually these terms are also required from holographic renormalization (see *e.g.* [44]). Of course in this paper we will not consider such counterterms and those needed due to null boundaries [45].

The aim of this article is to compute on-shell action on certain subregions behind and outside the horizon enclosed by null boundaries. We will consider an eternal black brane that provides a gravitational dual for a thermofield double state. Those subregions that are behind the horizon are UV finite and time dependent, though those outside the horizon are typically UV divergent and time independent.

To proceed we will consider a  $(d+2)$ -dimensional black brane solution in Einstein gravity whose metric is<sup>3</sup>

$$ds^2 = \frac{L^2}{r^2} \left( -f(r)dt^2 + \frac{dr^2}{f(r)} + \sum_{i=1}^d d\vec{x}^2 \right), \quad f(r) = 1 - \left( \frac{r}{r_h} \right)^{d+1}, \quad (1.4)$$

where  $r_h$  is the radius of horizon and  $L$  denotes the AdS radius. In terms of these parameters the entropy, mass and Hawking temperature of the corresponding black brane are

$$S_{th} = \frac{V_d L^d}{4G_N r_h^d}, \quad M = \frac{V_d L^d}{16\pi G_N} \frac{d}{r_h^{d+1}}, \quad T = \frac{d+1}{4\pi r_h}, \quad (1.5)$$

with  $V_d$  being the volume of  $d$ -dimensional internal space of the metric parametrized by  $x_i, i = 1, \dots, d$ . It is also useful to note that

$$\sqrt{-g} (R - 2\Lambda) = -2(d+1) \frac{L^d}{r^{d+2}}. \quad (1.6)$$

The organization of the paper is as follows. In the next section we will consider on-shell action on the WDW patch that using CA proposal may be related to the holographic complexity of the dual state. Our main concern is to present a closed form for the on-shell action. We will also compute on-shell action for past patch that is obtained by continuing the past null boundaries all the way to the past singularity. We will also compute on-shell action on the intersection of WDW patch with past and future interiors. We study the time evolution of holographic uncomplexity too. In section three we will consider different patches that are outside the horizon. This includes the intersection of WDW patch with entanglement wedge that could thought of as CA subregion complexity. The last

---

<sup>3</sup>Due to flat boundary of the black brane solution, we will be able to present our results in simple compact forms.

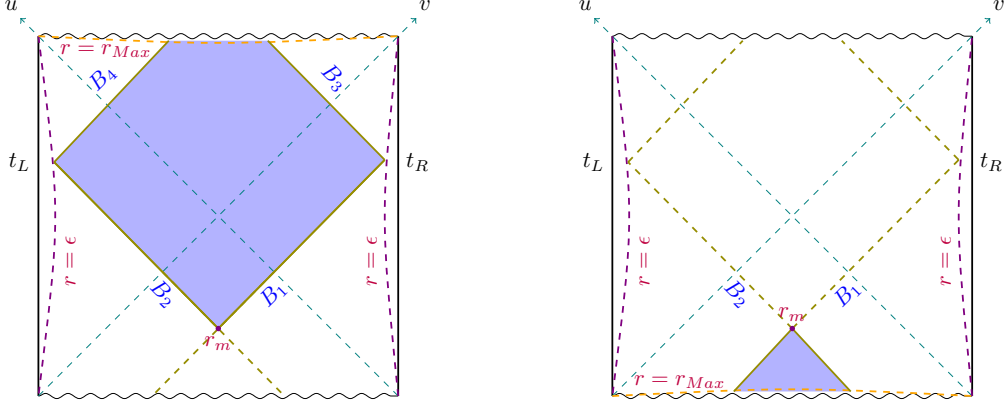


Figure 1: Penrose diagram of the WDW patch of an eternal AdS black hole assuming  $t_R = t_L$ . *Left*: WDW patch on which the on-shell action is computed to find the complexity. *Right*: Past patch corresponding to the WDW patch. The past patch may be identified as a part that is casually connected to an operator localized at  $r = r_m$  behind the horizon.

section is devoted to discussion and conclusion where we present the interpretation of our results.

## 2 Complexity and Subregions Behind the Horizon

### 2.1 CA Proposal

In this section using CA proposal we would like to evaluate complexity for the eternal two sided black brane which is dual to the thermofield double state in the boundary theory. Holographically one should compute on-shell action on WDW patch as depicted in the left panel of figure 1. Using the symmetry of the Penrose diagram of the eternal black hole, we shall consider a symmetric configuration with times  $t_R = t_L = \frac{\tau}{2}$ . Actually this question has been already addressed [18] where the full time dependence of complexity has been obtained where it was shown that the holographic complexity violates the Lloyd's bound in this case<sup>4</sup>. Of course our main interest in the present paper is to study the finite part of the on-shell action. In this subsection we will present the results and computations rather in details. Due to the similarity of computations, in the rest of the paper the computations will be a little bit brief.

To proceed we note that the null boundaries of the corresponding WDW patch are (see left panel of figure 1)

$$\begin{aligned} B_1 : t &= t_R - r^*(\epsilon) + r^*(r), & B_2 : t &= -t_L + r^*(\epsilon) - r^*(r), \\ B_3 : t &= t_R + r^*(\epsilon) - r^*(r), & B_4 : t &= -t_L - r^*(\epsilon) + r^*(r), \end{aligned} \quad (2.1)$$

<sup>4</sup>The one sided black hole was also discussed in [20, 41–43] where it confirmed that in this case the Lloyd's bound is respected.

by which the position of the joint point  $m$  is given by<sup>5</sup>

$$\tau \equiv t_L + t_R = 2(r^*(\epsilon) - r^*(r_m)). \quad (2.2)$$

Let us now compute the on-shell action over the corresponding WDW patch. As we already mentioned the action consists of several parts that include bulk, boundaries and joint actions. Using equation (1.6) the bulk action is [18]

$$I_{\text{WDW}}^{\text{bulk}} = -\frac{V_d L^d}{4\pi G_N} (d+1) \left( 2 \int_{\epsilon}^{r_{\text{Max}}} \frac{dr}{r^{d+2}} (r^*(\epsilon) - r^*(r)) + \int_{r_m}^{r_{\text{Max}}} \frac{dr}{r^{d+2}} \left( \frac{\tau}{2} - r^*(\epsilon) + r^*(r) \right) \right). \quad (2.3)$$

By making use of an integration by parts the above bulk action reads

$$\begin{aligned} I_{\text{WDW}}^{\text{bulk}} &= -\frac{V_d L^d}{4\pi G_N} \left( 2 \int_{\epsilon}^{r_{\text{Max}}} \frac{dr}{r^{d+1} f(r)} - \int_{r_m}^{r_{\text{Max}}} \frac{dr}{r^{d+1} f(r)} \right) \\ &= -\frac{V_d L^d}{4\pi G_N} \left( \frac{\tau + \tau_c}{2r_h^{d+1}} + \frac{2}{d\epsilon^d} - \frac{1}{dr_m^d} \right), \end{aligned} \quad (2.4)$$

where  $\tau_c = 2(r^*(\epsilon) - r^*(r_{\text{Max}}))$  is the critical time below which the time derivative of complexity vanishes [4, 18]. More explicitly one has (see also [18])

$$\tau_c = \frac{1}{2T} \frac{1}{\sin \frac{\pi}{d+1}}. \quad (2.5)$$

To find the boundary contributions we note that using the affine parametrization for the null directions, the corresponding boundary terms vanish<sup>6</sup> and we are left with just a spacelike boundary at future singularity whose contribution is given by

$$I_{\text{WDW}}^{\text{surf}} = -\frac{1}{8\pi G_N} \int d^d x \int_{-t_L - r^*(\epsilon) + r^*(r)}^{t_R + r^*(\epsilon) - r^*(r)} dt \sqrt{h} K_s \Big|_{r=r_{\text{Max}}}, \quad (2.6)$$

where  $K_s$  is the trace of extrinsic curvature of the boundary at  $r = r_{\text{Max}}$  and  $h$  is the determinant of the induced metric. To compute this term it is useful to note that for a constant  $r$  surface using the metric (1.4) one has

$$\sqrt{h} K = -\sqrt{g^{rr}} \partial_r \sqrt{h} = -\frac{1}{2} \frac{L^d}{r^d} \left( \partial_r f(r) - \frac{2(d+1)}{r} f(r) \right). \quad (2.7)$$

---

<sup>5</sup>Note that in our notation one has  $r^*(r) \leq 0$ .

<sup>6</sup>For affine parametrization of the null direction, the extrinsic curvature of the null boundary will be zero and therefore there is no contribution from null boundaries. In this paper we always use this parametrization and therefore we do not need to consider the boundary terms for null boundaries.

Plugging the above expression into (2.6) and evaluating it at  $r = r_{\text{Max}}$  one finds

$$I_{\text{WDW}}^{\text{surf}} = \frac{V_d L^d}{8\pi G_N} (d+1) \frac{\tau + \tau_c}{2r_h^{d+1}}. \quad (2.8)$$

There are also several joint points which may contribute to the on-shell action. Two of them are located at the future singularity that have zero contributions, while the contributions of the three remaining points at  $r = \epsilon$  and  $r = r_m$  are given by

$$I_{\text{WDW}}^{\text{joint}} = 2 \times \frac{-1}{8\pi G_N} \int_{\epsilon} d^d x \sqrt{\gamma} \log \frac{|k_1 \cdot k_2|}{2} + \frac{1}{8\pi G_N} \int_{r_m} d^d x \sqrt{\gamma} \log \frac{|k_1 \cdot k_2|}{2}, \quad (2.9)$$

where the factor of 2 is due to the two joint points at  $r = \epsilon$  for left and right boundaries. Here  $k_1$  and  $k_2$  are the null vectors associated with the null boundaries

$$k_1 = \alpha \left( -dt + \frac{dr}{f(r)} \right), \quad k_2 = \beta \left( dt + \frac{dr}{f(r)} \right). \quad (2.10)$$

Here  $\alpha$  and  $\beta$  are two constants appearing due to the ambiguity of the normalization of normal vectors of null segments. Therefore one gets

$$I_{\text{WDW}}^{\text{joint}} = -\frac{V_d L^d}{4\pi G_N} \frac{\log \frac{\alpha\beta\epsilon^2}{L^2}}{\epsilon^d} + \frac{V_d L^d}{8\pi G_N} \left( \frac{\log \frac{\alpha\beta r_m^2}{L^2}}{r_m^d} - \frac{\log |f(r_m)|}{r_m^d} \right). \quad (2.11)$$

It is clear from the above expression that the result suffers from an ambiguity associated with the normalization of null vectors. This ambiguity may be fixed either by fixing the constants  $\alpha$  and  $\beta$  by hand or adding a proper term to the action. Actually as we have already mentioned in order to maintain the diffeomorphism invariance of the action we will have to add another term given by equation (1.2). Note that even with this term we are still left with an undetermined free parameter. In the present case taking into account all four null boundaries one gets<sup>7</sup>

$$I_{\text{WDW}}^{\text{amb}} = -\frac{V_d L^d}{8\pi G_N} \left( \frac{\log \frac{\alpha\beta \tilde{L}^2 r_m^2}{L^4}}{r_m^d} + \frac{2}{d r_m^d} \right) + \frac{V_d L^d}{4\pi G_N} \left( \frac{\log \frac{\alpha\beta \tilde{L}^2 \epsilon^2}{L^4}}{\epsilon^d} + \frac{2}{d \epsilon^d} \right). \quad (2.12)$$

Now we have all terms in the action evaluated on the WDW patch. Therefore one arrives at

$$\begin{aligned} I_{\text{WDW}} &= I^{\text{bulk}} + I^{\text{surf}} + I^{\text{joint}} + I^{\text{amb}} \\ &= \frac{V_d L^d}{8\pi G_N} \left[ \frac{2}{\epsilon^d} \log \frac{\tilde{L}^2}{L^2} + \frac{d-1}{2r_h^{d+1}} (\tau + \tau_c) - \frac{\log \frac{\tilde{L}^2 |f(r_m)|}{L^2}}{r_m^d} \right]. \end{aligned} \quad (2.13)$$

It is important to note that in order to have a meaningful result the divergent term should be

---

<sup>7</sup> Note that for boundary associated with  $k_1$  one has  $\frac{dr}{d\lambda} = \alpha \frac{r^2}{L^2}$  and  $\Theta = 2d\alpha \frac{r}{L^2}$ . For the other null vector one should replace  $\alpha$  with  $\beta$ .

positive that is the case for  $\tilde{L} \geq L$ . On the other hand setting  $\tilde{L} = L$  the divergent term will drop and one gets a finite result consisting of two contributions<sup>8</sup>: one from the future spacelike singularity and a contribution from the joint point at  $r = r_m$  given as follows

$$I_{\text{WDW}} = \frac{V_d L^d}{8\pi G_N} \left[ \frac{d-1}{2r_h^{d+1}} (\tau + \tau_c) - \frac{\log |f(r_m)|}{r_m^d} \right]. \quad (2.14)$$

It is also interesting to note that for  $r_m \rightarrow r_{Max}$  where  $\tau \rightarrow \tau_c$  one gets

$$I_{\text{WDW}} = \frac{V_d L^d}{8\pi G_N} \frac{d-1}{r_h^{d+1}} \tau_c = \frac{d-1}{d+1} \frac{S_{th}}{\sin \frac{\pi}{d-1}}, \quad (2.15)$$

which is identically zero for  $d = 1$ . This might be thought of as complexity of formation of the black brane [46]. On the other hand, using the fact that  $\log |f(r_m)| \approx -\frac{(d+1)\tau}{2r_h}$  for  $r_m \rightarrow r_h$  (see next section), one gets linear growth at late times

$$I_{\text{WDW}} \approx \frac{V_d L^d}{8\pi G_N} \frac{d}{r_h^{d+1}} \tau = 2M\tau, \quad (2.16)$$

as expected.

## 2.2 Past Patch

In this subsection we would like to compute on-shell action on the past patch defined by the colored triangle shown in the right panel of figure 1. Clearly the rate of change of on-shell action on the past patch is the same as that of the WDW patch. Another way to think of the past patch is to consider an operator localized at  $r = r_m$  behind the horizon. The part of spacetime that can be causally connected to the operator is the triangle depicted in figure 1. Following CA proposal one may think of the on-shell action evaluated on the past patch as the complexity associated with the operator.

Let us compute the on-shell action for the past patch. To proceed we note that using the notation of the previous subsection the contribution of the bulk term to the on-shell action is

$$\begin{aligned} I_{\text{past}}^{\text{bulk}} &= -\frac{V_d L^d}{8\pi G_N} (d+1) \int_{r_m}^{r_{Max}} \frac{dr}{r^{d+2}} \int_{-t_L + r^*(0) - r^*(r)}^{t_R - r^*(0) + r^*(r)} dt \\ &= \frac{V_d L^d}{4\pi G_N} \int_{r_m}^{r_{Max}} \frac{dr}{r^{d+1} f} = \frac{V_d L^d}{4\pi G_N} \left( \frac{\tau - \tau_c}{2r_h^{d+1}} + \frac{1}{dr_m^d} \right). \end{aligned} \quad (2.17)$$

---

<sup>8</sup>Actually in the context of holographic renormalization one would add certain counterterms to make on-shell action finite. In the present case to remove the divergent term one may add a counterterm in the following form

$$I^{\text{ct}} = \frac{1}{8\pi G_N} \int d\lambda d^d x \sqrt{\gamma} \Theta \log \frac{L^2}{\tilde{L}^2},$$

which is essentially equivalent to set  $\tilde{L} = L$  and then we are left with finite on-shell action. Of course in this paper we keep the length scale  $\tilde{L}$  undetermined.



Here to get the second line we have performed an integration by parts. On the other hand the contribution of the spacelike boundary at past singularity is found to be

$$I_{\text{past}}^{\text{surf}} = \frac{1}{8\pi G_N} \int d^d x \int_{-t_L + r^*(0) - r^*(r)}^{t_R - r^*(0) + r^*(r)} dt \sqrt{h} K_s \Big|_{r=r_{\text{Max}}} = \frac{V_d L^d}{8\pi G_N} (d+1) \frac{\tau - \tau_c}{2r_h^{d+1}}. \quad (2.18)$$

There are also three joint points two of which at  $r = r_{\text{Max}}$  and one at  $r = r_m$ . The corresponding contributions to the on-shell action for those at  $r_{\text{Max}}$  vanish for large  $r_{\text{Max}}$ , while the contribution of that at  $r = r_m$  is given by

$$I_{\text{past}}^{\text{joint}} = \frac{1}{8\pi G_N} \int d^{d-1} x \sqrt{\gamma} \log \frac{|k_1 \cdot k_2|}{2} = \frac{V_d L^d}{8\pi G_N} \left( \frac{\log \frac{\alpha \beta r_m^2}{L^2}}{r_m^d} - \frac{\log |f(r_m)|}{r_m^d} \right). \quad (2.19)$$

Finally the contribution of term needed to remove the ambiguity is

$$I_{\text{past}}^{\text{amb}} = -\frac{V_d L^d}{8\pi G_N} \left( \frac{\log \frac{\alpha \beta \tilde{L}^2 r_m^2}{L^4}}{r_m^d} + \frac{2}{d r_m^d} \right). \quad (2.20)$$

Therefore altogether one arrives at

$$I_{\text{past}} = \frac{V_d L^d}{8\pi G_N} \left( \frac{d-1}{2r_h^{d+1}} (\tau - \tau_c) - \frac{\log \frac{\tilde{L}^2 |f(r_m)|}{L^2}}{r_m^d} \right), \quad (2.21)$$

which is UV finite even with arbitrary finite length scale  $\tilde{L}$ . Note that for  $r_m \rightarrow r_{\text{Max}}$  where  $\tau \rightarrow \tau_c$  the on-shell action for past patch vanishes identically. On the other hand, in the late times where  $r_m \rightarrow r_h$  one finds linear growth as expected.

### 2.3 Intersection of WDW Patch with Past and Future Interiors

Even for a static geometry, such as eternal black hole, the interior of black hole grows with time indicating that there could be a quantity in the dual field theory that grows with time far after the system reaches the thermal equilibrium. Indeed this was the original motivation for holographic computational complexity to be identified with the volume of the black hole interior.

In the previous subsection we have computed the on-shell action over whole WDW patch. The aim of this subsection is to compute on-shell action in the intersection of WDW patch with black brane interior. This consists of past and future interiors as shown in figure 2. Actually these subregions are the main parts that contribute to the time dependence of complexity of the dual state. It is, however, instructive to study these parts separately.<sup>9</sup>

---

<sup>9</sup>On-shell action for subregion in the black hole interior has been also studied in [47] where it was argued that complexity may be used as a probe to study the nature of different singularities.

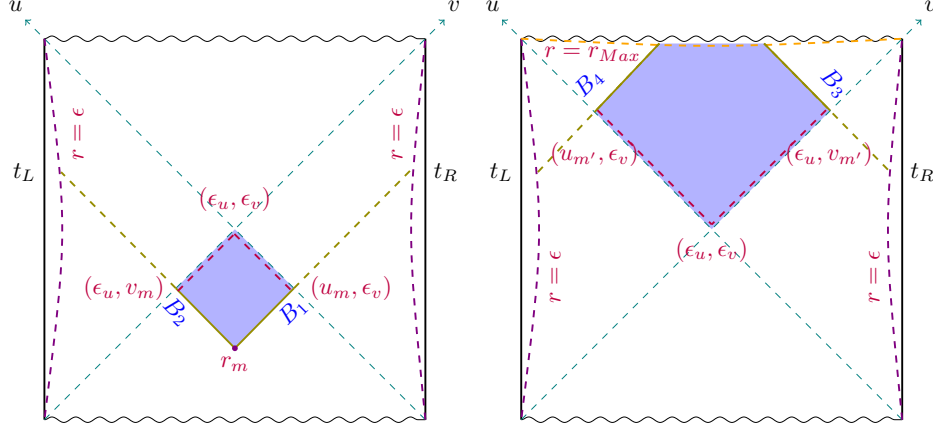


Figure 2: *Left*: Intersection of WDW patch with the past interior. *Right*: Intersection of WDW patch with the future interior.

### 2.3.1 Past Interior

To begin with we first consider the intersection of WDW patch with past interior as shown in the left panel of figure 2. Actually one may use the results of the previous subsection to write different terms contributing to the on-shell action. To start with we note that for the bulk term one has

$$I_{\text{PI}}^{\text{bulk}} = \frac{V_d L^d}{4\pi G_N} (d+1) \int_{r_h}^{r_m} \frac{dr}{r^{d+2}} \left( \frac{\tau}{2} - r^*(\epsilon) + r^*(r) \right) = \frac{V_d L^d}{4\pi G_N} \left( \frac{1}{d r_m^d} - \frac{1}{d r_h^d} \right). \quad (2.22)$$

There are four joint points, one at  $r = r_m$  and three at  $r = r_h$  that contribute to the on-shell action. It is, however, important to note that those points at the horizon are not at the same point. In other words the radial coordinate  $r$  is not suitable to make a distinction between these points. Indeed to distinguish between these points, following [48], it is convenient to use the following coordinate system for the past interior

$$u = -e^{-\frac{1}{2}f'(r_h)(r^*(r)-t)}, \quad v = -e^{-\frac{1}{2}f'(r_h)(r^*(r)+t)}. \quad (2.23)$$

In this coordinate system the horizon is located at  $uv = 0$  (*i.e.*  $r^*(r_h) = -\infty$ ). This equation has three nontrivial solutions given by  $(u = 0, v \neq 0)$ ,  $(u \neq 0, v = 0)$  and  $(u = 0, v = 0)$  that correspond to three joint points at the horizon shown in figure 2. Since both  $r^*(r)$  and  $\log f(r)$  are singular at  $r = r_h$ , one may regularize the contribution of these three points by setting the horizon at  $v = \epsilon_v$  and  $u = \epsilon_u$ . In this notation the joint points are given by  $(\epsilon_u, v_m)$ ,  $(u_m, \epsilon_v)$  and  $(\epsilon_u, \epsilon_v)$  as depicted in figure 2. In what follows the radial coordinate associated with these three points are denoted by

$r_{v_m}, r_{u_m}$  and  $r_\epsilon$ , respectively. Using this notation the contribution of joint points is

$$\begin{aligned} I_{\text{PI}}^{\text{joint}} &= \frac{V_d L^d}{8\pi G_N} \left( \frac{\log \frac{\alpha \beta r_m^2}{L^2 |f(r_m)|}}{r_m^d} - \frac{\log \frac{\alpha \beta r_{u_m}^2}{L^2 |f(r_{u_m})|}}{r_{u_m}^d} - \frac{\log \frac{\alpha \beta r_{v_m}^2}{L^2 |f(r_{v_m})|}}{r_{v_m}^d} + \frac{\log \frac{\alpha \beta r_\epsilon^2}{L^2 |f(r_\epsilon)|}}{r_\epsilon^d} \right) \\ &= -\frac{V_d L^d}{8\pi G_N} \left( \frac{\log |f(r_m)|}{r_m^d} + \frac{\log |f(r_\epsilon)| - \log |f(r_{u_m})| - \log |f(r_{v_m})|}{r_h^d} + \frac{\log \frac{\alpha \beta r_h^2}{L^2}}{r_h^d} - \frac{\log \frac{\alpha \beta r_m^2}{L^2}}{r_m^d} \right). \end{aligned} \quad (2.24)$$

Here we have used the fact that  $\{r_{u_m}, r_{v_m}, r_\epsilon\} \approx r_h$ . On the other hand by making use of the fact that [48]

$$\log |f(r_{u,v})| = \log |uv| + c_0 + \mathcal{O}(uv) \quad \text{for } uv \rightarrow 0, \quad (2.25)$$

one gets

$$\begin{aligned} \log |f(r_{u_m})| &= \log |u_m \epsilon_v| + c_0 + \mathcal{O}(\epsilon_v), \\ \log |f(r_{v_m})| &= \log |\epsilon_u v_m| + c_0 + \mathcal{O}(\epsilon_u), \\ \log |f(r_\epsilon)| &= \log |\epsilon_u \epsilon_v| + c_0 + \mathcal{O}(\epsilon_u \epsilon_v), \end{aligned} \quad (2.26)$$

which can be used to simplify (2.24) as follows

$$I_{\text{PI}}^{\text{joint}} = -\frac{V_d L^d}{8\pi G_N} \left( \frac{\log |f(r_m)|}{r_m^d} - \frac{\log(u_m v_m) + c_0}{r_h^d} + \frac{\log \frac{\alpha \beta r_h^2}{L^2}}{r_h^d} - \frac{\log \frac{\alpha \beta r_m^2}{L^2}}{r_m^d} \right). \quad (2.27)$$

Here  $c_0 = \psi^{(0)}(1) - \psi^{(0)}(\frac{1}{d+1})$  is a positive number and  $\psi^{(0)}(x) = \frac{\Gamma'(x)}{\Gamma(x)}$  is the digamma function.

Finally one has to remove the ambiguity due to the normalization of the null vectors by adding the extra term (1.2) to the action. The resulting expression is then

$$I_{\text{PI}}^{\text{amb}} = -\frac{V_d L^d}{8\pi G_N} \left( \frac{\log \frac{\alpha \beta \tilde{L}^2 r_m^2}{L^4}}{r_m^d} + \frac{2}{d r_m^d} \right) + \frac{V_d L^d}{8\pi G_N} \left( \frac{\log \frac{\alpha \beta \tilde{L}^2 r_h^2}{L^4}}{r_h^d} + \frac{2}{d r_h^d} \right). \quad (2.28)$$

Therefore altogether for the subregion given by the intersection of the WDW patch with the past interior shown in the left panel of figure 2 one gets

$$I_{\text{PI}} = \frac{V_d L^d}{8\pi G_N} \left( \frac{1}{r_h^d} \log \frac{\tilde{L}^2}{L^2} + \frac{c_0}{r_h^d} - \frac{(d+1)\tau}{2r_h^{d+1}} - \frac{\log \frac{\tilde{L}^2 |f(r_m)|}{L^2}}{r_m^d} \right), \quad (2.29)$$

which depends on time through its  $r_m$  dependence, as expected. Here we have used the fact that  $\log(u_m v_m) = -f'(r_h) r^*(r_m) = -\frac{(d+1)\tau}{2r_h}$ . Note that for  $r_m \rightarrow r_{\text{Max}}$  the time dependence of the

on-shell action drops out resulting to

$$I_{\text{PI}} = \left( c_0 - \frac{(d+1)\tau_c}{2r_h} + \log \frac{\tilde{L}^2}{L^2} \right) \frac{S_{th}}{2\pi}. \quad (2.30)$$

Note also that at late times where  $r_m \rightarrow r_h$ , using equation (2.25), the total on-shell action in the past interior vanishes.

### 2.3.2 Future Interior

Let us now compute on-shell action for the intersection of the WDW patch with the future interior shown in the right panel of figure 2. In this case, using our previous results, the bulk term of the action is

$$I_{\text{FI}}^{\text{bulk}} = -\frac{V_d L^d}{4\pi G_N} (d+1) \int_{r_h}^{r_{Max}} \frac{dr}{r^{d+2}} \left( \frac{\tau}{2} + r^*(\epsilon) - r^*(r) \right) = -\frac{V_d L^d}{4\pi G_N} \left( \frac{1}{d r_h^d} + \frac{\tau + \tau_c}{2 r_h^{d+1}} \right). \quad (2.31)$$

There are five joint points two of which have zero contributions for large  $r_{Max}$ , while the contributions of other three points are given by

$$\begin{aligned} I_{\text{FI}}^{\text{joint}} &= \frac{V_d L^d}{8\pi G_N} \left( \frac{\log \frac{\alpha\beta r_\epsilon^2}{L^2 |f(r_\epsilon)|}}{r_\epsilon^d} - \frac{\log \frac{\alpha\beta r_{u_{m'}}^2}{L^2 |f(r_{u_{m'}})|}}{r_{u_{m'}}^d} - \frac{\log \frac{\alpha\beta r_{v_{m'}}^2}{L^2 |f(r_{v_{m'}})|}}{r_{v_{m'}}^d} \right) \\ &= -\frac{V_d L^d}{8\pi G_N} \left( \frac{\log |f(r_\epsilon)| - \log |f(r_{u_{m'}})| - \log |f(r_{v_{m'}})|}{r_h^d} + \frac{\log \frac{\alpha\beta r_h^2}{L^2}}{r_h^d} \right) \\ &= \frac{V_d L^d}{8\pi G_N} \left( \frac{\log |u_{m'} v_{m'}| + c_0}{r_h^d} - \frac{\log \frac{\alpha\beta r_h^2}{L^2}}{r_h^d} \right). \end{aligned} \quad (2.32)$$

The boundary terms associated with the null boundaries vanish using affine parametrization for the null directions and the only term we need to compute is the surface term at future singularity. This is indeed the term we have already computed in (2.8)

$$I_{\text{FI}}^{\text{surf}} = \frac{V_d L^d}{8\pi G_N} (d+1) \frac{\tau + \tau_c}{2 r_h^{d+1}}. \quad (2.33)$$

The only remaining contribution to be computed is the term needed to remove the ambiguity

$$I_{\text{FI}}^{\text{amb}} = \frac{V_d L^d}{8\pi G_N} \left( \frac{\log \frac{\alpha\beta \tilde{L}^2 r_h^2}{L^4}}{r_h^d} + \frac{2}{d r_h^d} \right). \quad (2.34)$$

Taking all terms into account we have

$$I_{\text{FI}} = \frac{V_d L^d}{8\pi G_N} \left( \frac{d\tau}{r_h^{d+1}} + \frac{(d-1)\tau_c}{2r_h^{d+1}} + \frac{c_0}{r_h^d} + \frac{1}{r_h^d} \log \frac{\tilde{L}^2}{L^2} \right). \quad (2.35)$$

Here to get the final result we have used the fact that  $\log |u_{m'} v_{m'}| = \frac{(d+1)\tau}{2r_h}$ .

It is also interesting to sum the contributions of both regions shown in figure 2 and compare the resultant expression with the on-shell action evaluated on the whole WDW patch

$$I_{\text{Ext}} = I_{\text{WDW}} - (I_{\text{PI}} + I_{\text{FI}}) = 2 \times \frac{V_d L^d}{8\pi G_N} \left[ -\frac{c_0}{r_h^d} + \left( \frac{1}{\epsilon^d} - \frac{1}{r_h^d} \right) \log \frac{\tilde{L}^2}{L^2} \right]. \quad (2.36)$$

that is time independent, as expected. In fact this is the contribution of the part of the WDW patch that is outside of the black hole horizon. The factor of two is a symmetric factor between left and right sides of the corresponding WDW patch. It is also interesting to note that the finite term is negative! We will consider the above result in the next section where we will study subregion complexity.

## 2.4 Late Time Behavior

In this section we will study the time derivative of the on-shell actions we have found in the previous subsections. To proceed we note that from definitions of  $r^*$  and  $r_m$  one has

$$\frac{dr^*(r_m)}{d\tau} = -\frac{1}{2}, \quad \frac{dr_m}{d\tau} = \frac{1}{2} f(r_m), \quad (2.37)$$

which can be used to show

$$\frac{dI_{\text{WDW}}}{d\tau} = \frac{dI_{\text{past}}}{d\tau} = 2M \left( 1 + \frac{1}{2} \tilde{f}(r_m) \log \frac{\tilde{L}^2 |f(r_m)|}{L^2} \right), \quad \tilde{f} = \frac{r_h^{d+1}}{r_m^{d+1}} - 1. \quad (2.38)$$

It is also interesting to compute the time derivative of the on-shell action for the individual subregions we have considered before. Actually it is straightforward to see

$$\frac{dI_{\text{PI}}}{d\tau} = M \tilde{f}(r_m) \log \frac{\tilde{L}^2 |f(r_m)|}{L^2}, \quad \frac{dI_{\text{FI}}}{d\tau} = 2M, \quad \frac{dI_{\text{Ext}}}{d\tau} = 0. \quad (2.39)$$

It is evident that summing up these contributions one gets (2.38), as expected. Note that at late times where  $r_m \rightarrow r_h$ , the past interior has no contribution to the rate of complexity growth.

Of course it is known that the complexity obtained from WDW patch violates the Lloyd's bound, though at late time it approaches  $2M$ . From the above results it is evident that the contribution to the late time behavior comes from the future interior of the black brane. It is also worth noting that the violation of the Lloyd's bound is due to the contribution of the joint point located at the past interior. This, in turns, suggests that if one defines the complexity as on-shell action on the intersection of WDW patch and future interior the resultant complexity fulfills the bound and has

linear growth all the time! Of course if one wants appropriate UV divergences before regularizing the complexity we should also add the contributions of the exterior region too. More explicitly one has

$$\tilde{I}_{\text{WDW}} = I_{FI} + I_{\text{Ext}} = 2M \left( \tau + \frac{(d-1)\tau_c - 2c_0 r_h}{d} + \left( \frac{2r_h^{d+1}}{d\epsilon^d} - \frac{r_h}{d} \right) \log \frac{\tilde{L}^2}{L^2} \right). \quad (2.40)$$

It is also instructive to note that at late time where  $r_m \rightarrow r_h$ , setting  $r_m - r_h = \xi$ , from equation (2.2) one finds

$$\tau = -\frac{2r_h}{d+1} \left( \log \frac{(d+1)\xi}{r_h} - c_0 \right) \sim \frac{\beta}{2\pi} \log \frac{r_h}{(d+1)\xi}, \quad \text{with } \beta = \frac{1}{T}. \quad (2.41)$$

In particular when one is away from the horizon about a power of Planck scale  $\xi \sim \frac{\ell_p^d}{r_h^{d-1}}$  the above late time behavior reads

$$\tau \sim \frac{\beta}{2\pi} \log S_{th}, \quad (2.42)$$

in which the on-shell action reads  $I \sim S_{th} \log S_{th}$ , that is the scrambling complexity. Following [49] one may also consider the case where the time is about of  $\tau \sim \frac{\beta}{2\pi} e^{S_{th}}$  that could be the time where one gets maximum complexity. At that time the on-shell action is

$$I \sim S_{th} e^{S_{th}}, \quad (2.43)$$

which could be thought of maximum complexity of the system [49].

## 2.5 Holographic Uncomplexity

Given a time slice and the associated WDW patch one may want to compute on-shell action on a region that should be included in the WDW patch as time goes. The corresponding region is shown in figure 3. Actually following [49] one may identify the on-shell action on this region with “holographic uncomplexity” that is the gap between the complexity and the maximum possible complexity (see also [50, 51]). In other words the uncomplexity is a room for complexity to increase. Alternatively one could thought of the holographic uncomplexity as the spacetime resource available to an observer who intends to enter the horizon [49].

Clearly the on-shell action on the region depicted in figure 3 is given by a difference of on-shell action evaluated on the future interior

$$I_{\text{UC}} = I_{\text{FI}2} - I_{\text{FI}1} = 2M(\tau_2 - \tau_1). \quad (2.44)$$

where  $\tau$  is the actual boundary time. It is also important to note that  $\tau_2$  should be thought of a time cut off and eventually we are interested in  $\tau_2 \rightarrow \infty$  limit for some fixed  $\tau_1$ . Indeed the time cut off could be set to  $\tau_2 \sim \frac{\beta}{2\pi} e^{S_{th}}$ .

As we mentioned the holographic uncomplexity is defined as a difference between maximum

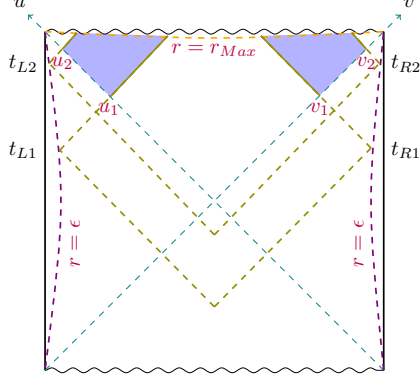


Figure 3: Spacetime region corresponding to evaluation of holographic uncomplexity. The regions shown by blue color compute uncomplexity given by the equation (2.44). This is not equal to difference between maximum complexity and the complexity of the state at a given time (see equation (2.46)).

complexity and the complexity of the state at a given time, it is then evident from (2.44) that this equation can not capture this difference. The crucial point is that the complexity, as we already mentioned, has two components: one from the boundary term and one from the joint point. The resultant uncomplexity given in equation (2.44) does not fully contain the contribution of joint point. To be precise using equation (2.13) one has

$$\begin{aligned} \Delta I_{\text{WDW}} &= I_2^{\text{WDW}} - I_1^{\text{WDW}} \\ &= \frac{V_d L^d}{8\pi G_N} \left[ \frac{d-1}{2r_h^{d+1}} (\tau_2 - \tau_1) - \frac{\log |f(r_{m2})|}{r_{m2}^d} + \frac{\log |f(r_{m1})|}{r_{m1}^d} \right]. \end{aligned} \quad (2.45)$$

One observes that there is a joint contribution that the subregion shown in figure 3 can not see it and thus it is not equal to  $I_{\text{UC}}$ . Of course it approaches  $I_{\text{UC}}$  when both  $r_{m1}$  and  $r_{m2}$  approach the horizon. Actually using the fact that  $\tau_2$  should be thought of a cut off and therefore it is large (*i.e.*  $r_{m2} \rightarrow r_h$ ) the above expression reads

$$\Delta I_{\text{WDW}} \approx 2M(\tau_2 - \tau_1) - \frac{V_d L^d}{8\pi G_N} \left[ \frac{c_0}{r_h^d} - \frac{(d+1)\tau_1}{2r_h^{d+1}} - \frac{\log |f(r_{m1})|}{r_{m1}^d} \right]. \quad (2.46)$$

Note that the second part is just the on-shell action evaluated on the past interior that vanishes as  $r_{m1}$  approaches the horizon. It is worth mentioning that, although it is not clear from this expression, setting  $\tau_1 = \tau_2$  the above equation vanishes. To see this we note that in this expression the time  $\tau_2$  is associated with the limit where  $r_{m2} \approx r_h$ . Therefore setting  $\tau_1 = \tau_2$  the joint point  $r_{m1}$  approaches the horizon too and thus the expression in the bracket vanishes in this limit as well.

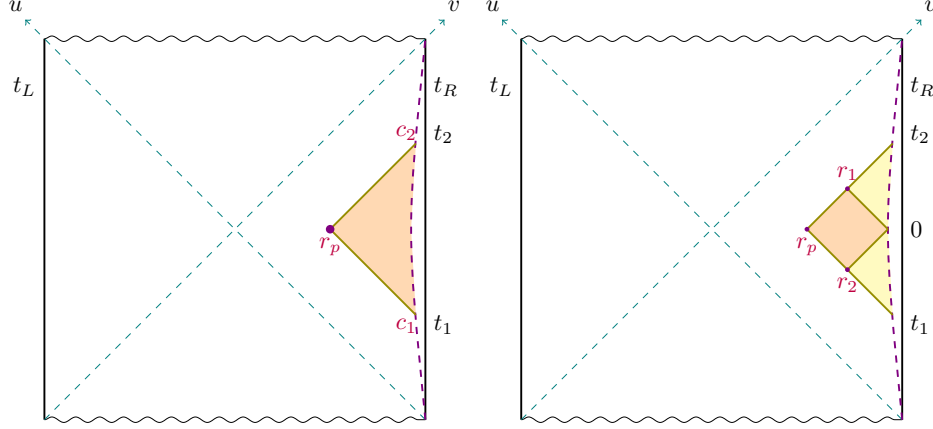


Figure 4: *Left:* A localized operator at  $P$ . The colored region is the part that is involved in the construction of the operator localized at  $r = r_p$ . *Right:* The orange region is the intersection of WDW patch and entanglement wedge at time slice  $t_R = 0$  for half of an eternal black hole.

### 3 Subregion Complexity and Outside the Horizon

In the previous section we have computed on-shell action on different regions containing a part that is located behind the horizon. These regions could be found by the intersection of a WDW patch with the interior of a two sided black brane. We have seen that the resultant on shell action is time dependent whenever it receives a contribution from a region inside the black brane.

On the other hand one may consider cases where the subregions of interest are entirely outside the horizon. This is, indeed, what we would like to consider in this section. In this case, unlike the previous cases, one usually gets time independent on shell action. In some case the region of interest could be thought of as intersection of the WDW patch with entanglement wedge.

#### 3.1 Complexity of Layered Stretched Horizon

Let us consider a subregion in the black hole exterior in the shape of a triangle shown in the left panel of figure 4. The three faces of the corresponding triangle are given by two null and a timelike boundaries

$$t = t_1 + r^*(\epsilon) - r^*(r), \quad t = t_2 - r^*(\epsilon) + r^*(r), \quad r = \epsilon. \quad (3.1)$$

The null boundaries intersect at the point  $r = r_p$  that is given by

$$\tilde{\tau} \equiv t_{R2} - t_{R1} = 2(r^*(\epsilon) - r^*(r_p)). \quad (3.2)$$

where  $\tilde{\tau}$  is the time interval. This should not be confused with the actual field theory time coordinate  $\tau$  we have used in the previous section.

Actually following [1] where the author has considered layered stretched horizon, this might be



thought of as a bulk operator  $P$  localized at point  $r_p$ . Indeed the corresponding triangle shows a region of the boundary involved in the construction of the operator  $P$ . Now the aim is to compute the on-shell action in this subregion. Following [1] the result might be thought of as complexity of the operator localized on the corresponding layer.

To proceed let us start with the bulk contribution. From the notation depicted in figure 4 it is straightforward to see

$$\begin{aligned} I_{\text{Tri}}^{\text{bulk}} &= -\frac{V_d L^d}{8\pi G_N} (d+1) \int_{\epsilon}^{r_p} \frac{dr}{r^{d+2}} (\tilde{\tau} - 2(r^*(\epsilon) - r^*(r))) \\ &= -\frac{V_d L^d}{8\pi G_N} \left( \frac{1}{\epsilon^{d+1}} - \frac{1}{r_h^{d+1}} \right) \tilde{\tau} + \frac{V_d L^d}{4\pi G_N d} \left( \frac{1}{\epsilon^d} - \frac{1}{r_p^d} \right). \end{aligned} \quad (3.3)$$

As for the boundary terms we only need to consider the Gibbons-Hawking-York term at the timelike boundary  $r = \epsilon$

$$I_{\text{Tri}}^{\text{surface}} = \frac{1}{8\pi G_N} \int d^d x \int_{t_1+r^*(\epsilon)-r^*(r)}^{t_2-r^*(\epsilon)+r^*(r)} dt \sqrt{h} K_t \Big|_{r=\epsilon} = \frac{(d+1)V_d L^d}{8\pi G_N} \left( \frac{1}{\epsilon^{d+1}} - \frac{1}{2r_h^{d+1}} \right) \tilde{\tau}. \quad (3.4)$$

The normal vectors associated with the boundaries of the triangle given by (3.1) are

$$n_t = \frac{L dr}{\epsilon \sqrt{f(\epsilon)}}, \quad k_1 = \alpha \left( -dt + \frac{dr}{f(r)} \right), \quad k_2 = \beta \left( dt + \frac{dr}{f(r)} \right), \quad (3.5)$$

which can be used to compute the contribution of the joint points as follows

$$\begin{aligned} I_{\text{Tri}}^{\text{joint}} &= \frac{1}{8\pi G_N} \int_{c_1} d^d x \sqrt{\gamma} \log |k_2 \cdot n_t| + \frac{1}{8\pi G_N} \int_{c_2} d^d x \sqrt{\gamma} \log |k_1 \cdot n_t| \\ &\quad - \frac{1}{8\pi G_N} \int_{r_p} d^d x \sqrt{\gamma} \log \left| \frac{k_1 \cdot k_2}{2} \right| \\ &= \frac{V_d L^d}{8\pi G_N} \frac{\log \frac{\alpha \beta \epsilon^2}{L^2}}{\epsilon^d} - \frac{V_d L^d}{8\pi G_N} \left( \frac{\log \frac{\alpha \beta r_p^2}{L^2}}{r_p^d} - \frac{\log f(r_p)}{r_p^d} \right). \end{aligned} \quad (3.6)$$

The contribution of the term needed to remove the ambiguity is

$$\begin{aligned} I_{\text{Tri}}^{\text{amb}} &= \frac{1}{8\pi G_N} \int_{\text{null}} d\lambda d^d x \sqrt{\gamma} \Theta \log \frac{|\tilde{L}\Theta|}{d} \\ &= \frac{V_d L^d}{8\pi G_N} \left( \frac{\log \frac{\alpha \beta \tilde{L}^2 r_p^2}{L^4}}{r_p^d} + \frac{2}{d r_p^d} \right) - \frac{V_d L^d}{8\pi G_N} \left( \frac{\log \frac{\alpha \beta \tilde{L}^2 \epsilon^2}{L^4}}{\epsilon^d} + \frac{2}{d \epsilon^d} \right). \end{aligned} \quad (3.7)$$

Therefore taking all contributions into account one arrives at

$$I_{\text{Tri}} = \frac{V_d L^d}{8\pi G_N} \left[ \left( \frac{d}{\epsilon^{d+1}} - \frac{d-1}{2r_h^{d+1}} \right) \tilde{\tau} + \left( \frac{1}{r_p^d} - \frac{1}{\epsilon^d} \right) \log \frac{\tilde{L}^2}{L^2} + \frac{\log f(r_p)}{r_p^d} \right]. \quad (3.8)$$

At this stage we would like to recall that whenever one is dealing with the computation of on shell action it is important to make it clear what one means by action. As we already mentioned by an action we mean all terms needed to have a covariant action with a well defined variational principle that result to a finite free energy. This, in particular, requires to consider the counter terms that obtained in the context of holographic renormalization. In the present case where we have a timelike flat boundary at  $r = \epsilon$ , the corresponding counterterm is given by

$$I_{\text{Tri}}^{\text{ct}} = -\frac{1}{8\pi G_N} \int_{r=\epsilon} d^{d+1}x \sqrt{h} \frac{d}{L}, \quad (3.9)$$

that gives the following contribution to the on shell action

$$I_{\text{Tri}}^{\text{ct}} = \frac{V_d L^d}{8\pi G_N} \left( -\frac{d}{\epsilon^{d+1}} + \frac{d}{2r_h^{d+1}} \right) \tilde{\tau}. \quad (3.10)$$

Combining the above result with equation (3.8), the total on-shell action reads<sup>10</sup>

$$I_{\text{Tri}} = \frac{V_d L^d}{8\pi G_N} \left[ -\frac{1}{\epsilon^d} \log \frac{\tilde{L}^2}{L^2} + \frac{\tilde{\tau}}{2r_h^{d+1}} + \frac{\log \frac{\tilde{L}^2 f(r_p)}{L^2}}{r_p^d} \right]. \quad (3.11)$$

Note that since we have already assumed  $\tilde{L} \geq L$ , from the above expression one finds that the most divergent term as well as the finite term are negative. This is of course in contrast with what one would expect from complexity. Actually the result is reminiscent of free energy of the black hole. Indeed denoting the contribution of joint point by  $\mathcal{J}$  one has (dropping the divergent term)

$$I_{\text{Tri}} = -\mathcal{F} \tilde{\tau} + \mathcal{J}_p \quad \text{with} \quad \mathcal{J}_p = \frac{\log f(r_p)}{r_p^d}, \quad (3.12)$$

where  $\mathcal{F} = -\frac{V_d L^d}{16\pi G_N} \frac{1}{r_h^{d+1}}$  is the free energy of the corresponding black brane. To summarize we note that the on-shell action in this case consists of two parts: the first part that might be thought of as the classical contribution is the contribution of the timelike boundary that is the free energy of corresponding black brane, while the second one that comes from joint point should be treated as the new contribution associated with the complexity of the operator. Clearly when a given subregion does not contain a timelike boundary the free energy drops and the whole contributions

---

<sup>10</sup> We note that the resultant on shell action is still divergent due to the ambiguity of fixing the length scale  $\tilde{L}$ . Of course there is a natural way to fix this length scale by assuming that the corresponding on shell action for an AdS geometry in the Poincare coordinates vanishes (as a reference state), leading to  $\tilde{L} = L$ . Therefore one ends up with a finite on shell action.

come from joint points (see next subsection).

For the case where the point  $r_p$  is in the vicinity of the horizon, *i.e.*,  $r_p = r_h - \xi$  for  $\xi \ll r_h$ , from equation (3.11) one finds

$$I_{\text{Tri}} \approx \frac{V_d L^d}{8\pi G_N} \left( \frac{1}{r_p^d} - \frac{1}{\epsilon^d} \right) \log \frac{\tilde{L}^2}{L^2} - \frac{V_d L^d}{16\pi G_N} \frac{1}{r_h^{d+1}} (d \tilde{\tau}). \quad (3.13)$$

that shows the layer (operator) becomes more complex as one approach the horizon. In particular when one is away from the horizon about the Planck length one gets

$$I_{\text{Tri}} \approx \frac{V_d L^d}{8\pi G_N} \left( \frac{1}{r_p^d} - \frac{1}{\epsilon^d} \right) \log \frac{\tilde{L}^2}{L^2} - \frac{1}{2\pi(d+1)} S_{th} \log S_{th} \quad (3.14)$$

### 3.2 CA Proposal and Subregion Complexity

An immediate application of the result we have obtained in the previous section is to find on-shell action for a square subregion shown in orange in the right panel of figure 4. The result may be used to compute on shell action on a region obtained by the intersection of entanglement wedge and WDW patch. The desired result can be found by algebraic summation of three triangles identified by  $r_1, r_2$  and  $r_p$ . Actually using equation (3.8) one gets<sup>11</sup>

$$\begin{aligned} I_{\text{Sq}} &= I_{r_p} - I_{r_1} - I_{r_2} \\ &= \frac{V_d L^d}{8\pi G_N} \left[ \left( \frac{1}{\epsilon^d} + \frac{1}{r_p^d} - \frac{1}{r_1^d} - \frac{1}{r_2^d} \right) \log \frac{\tilde{L}^2}{L^2} + \frac{\log f(r_p)}{r_p^d} - \frac{\log f(r_1)}{r_1^d} - \frac{\log f(r_2)}{r_2^d} \right]. \end{aligned} \quad (3.15)$$

Note that in this case the most divergent term is positive as expected for an expression representing complexity. Indeed since the corresponding subregion is the intersection of WDW patch and domain of dependence of a subregion in the boundary theory (which is the whole system in the present case at time  $\tau = 0$ ) we would like to identify this expression as the CA subregion complexity [8]. Note that since there is no timelike or spacelike boundaries, all contributions come from the joint points.

It is also interesting to consider the limit of  $\{r_p, r_1, r_2\} \rightarrow r_h$ , where we get a subregion shown in the left panel of figure 5. This is the intersection of WDW patch at time slice  $\tau = 0$  with the right exterior of the black hole. Actually by making use of equation (2.25) and with the notation shown in figure 5 in the limit of  $\{r_p, r_1, r_2\} \rightarrow r_h$ , equation (3.15) reads

$$I_{\text{Sq}} = \frac{V_d L^d}{8\pi G_N} \left( \frac{1}{\epsilon^d} - \frac{1}{r_h^d} \right) \log \frac{\tilde{L}^2}{L^2} - \frac{c_0}{2\pi} S_{th}. \quad (3.16)$$

It is important to note that although the most divergent term is positive for  $\tilde{L} > L$ , the finite term is negative. We note that on-shell action for the subregion shown in the left panel of figure 5 has

---

<sup>11</sup> One could have directly computed the on-shell action for the square region taking into account all terms in the action. Of course the result is the same as what we have found by an algebraic summation of three triangles.

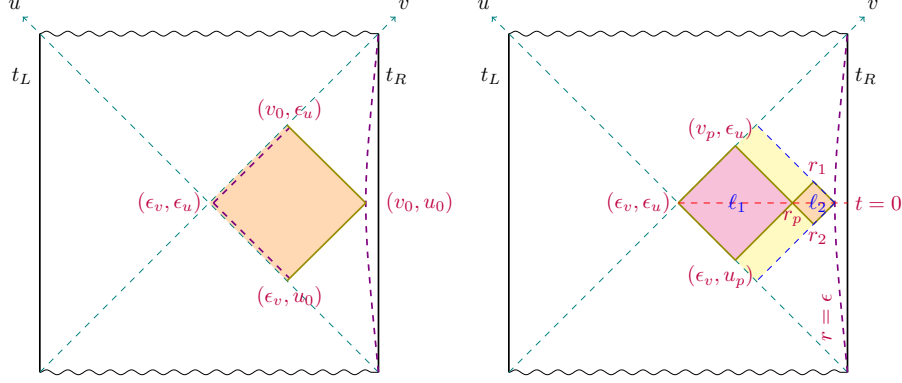


Figure 5: *Left*: Intersection of WDW patch and entanglement wedge for large entangling region at time slice  $t_R = 0$  for half of an eternal black hole. *Right*: Two subregions denoted by  $\ell_1$  and  $\ell_2$ .

been recently studied [48] where the authors have not considered the term needed to remove the ambiguity and have fixed the ambiguity by hand<sup>12</sup>. As a result the finite term they have found was positive. We note, however, that it is crucial to take into account the corresponding term to maintain the reparametrization invariance of the action. Note that for values of  $r_p$  it can be seen that the finite part of equation (3.15) is always negative<sup>13</sup>. It is also interesting to compare on-shell action evaluated on different subregions and union of the subregions. To proceed we will consider two subregions denoted by  $\ell_1$  and  $\ell_2$  in the right panel of figure 5. Using the notation shown in the figure and setting  $\tilde{L} = L$ , one has

$$\begin{aligned}
I_{\ell_1} &= \frac{V_d L^d}{8\pi G_N} \left( \frac{\log |f(r_p)|}{r_p^d} + \frac{\log |f(r_\epsilon)|}{r_h^d} - \frac{\log |f(r_{u_p})|}{r_h^d} - \frac{\log |f(r_{u_p})|}{r_h^d} \right) \\
&= \frac{V_d L^d}{8\pi G_N} \left( \frac{\log |f(r_p)|}{r_p^d} - \frac{c_0 + \log |u_p v_p|}{r_h^d} \right) = \frac{V_d L^d}{8\pi G_N} \left( \frac{\log |f(r_p)|}{r_p^d} - \frac{c_0 - f'(r_h) r^*(r_p)}{r_h^d} \right), \\
I_{\ell_2} &= \frac{V_d L^d}{8\pi G_N} \left( \frac{\log |f(r_p)|}{r_p^d} - \frac{\log |f(r_1)|}{r_1^d} - \frac{\log |f(r_2)|}{r_2^d} \right). \tag{3.17}
\end{aligned}$$

Here in order to simplify  $I_{\ell_1}$  we have used (2.25). On the other hand the on-shell action evaluated on  $\ell_1 \cup \ell_2$  is (3.16)

$$I_{\ell_1 \cup \ell_2} = -\frac{V_d L^d}{8\pi G_N} \frac{c_0}{r_h^d}. \tag{3.18}$$

Therefore one gets

$$A \equiv I_{\ell_1} + I_{\ell_2} - I_{\ell_1 \cup \ell_2} = \frac{V_d L^d}{8\pi G_N} \left( 2 \frac{\log |f(r_p)|}{r_p^d} - \frac{(d+1)r^*(r_p)}{r_h^{d+1}} - \frac{\log |f(r_1)|}{r_1^d} - \frac{\log |f(r_2)|}{r_2^d} \right). \tag{3.19}$$

<sup>12</sup>We note that the contribution of the term removing the ambiguity has been added to the published version of [48] where a proper citation to the present paper is also given.

<sup>13</sup>We would like to thank B. Swingle for discussions on this point.

It is then important to determine the sign of  $A$ . To do so, one first observes that  $A$  vanishes at both  $\{r_p, r_1, r_2\} \rightarrow r_h$  and  $\{r_p, r_1, r_2\} \rightarrow 0$  limits. On the other hand one can show that at  $\{r_p, r_1, r_2\} \approx 0$  the function  $A$  approaches zero from above leading to the fact that  $A \geq 0$ . This behavior may also be shown numerically. As a result we conclude that the on-shell action we have evaluated for subregions in the exterior of the black brane obeys subadditivity condition

$$I_{\ell_1} + I_{\ell_2} \geq I_{\ell_1 \cup \ell_2}, \quad (3.20)$$

that is indeed in agreement with results of [48] (see also [52]). It is worth noting that in order to reach the above result, the contribution of the corner term,  $\log u_p v_p$ , plays a crucial role.

## 4 Discussions and Conclusions

In this paper motivated by “complexity equals action” proposal we have evaluated on-shell action on certain spacetime subregions enclosed by null boundaries that of course includes the WDW patch itself too. Our main concern was to compute finite term of the on-shell action. It is contrary to the most studies in the literature where the main concern was to compute the growth rate of the complexity (see for example [53–66]).

Although we have computed on-shell action on a given subregion, taking into account all terms needed to have reparametrization invariance and well-defined variational principle, we have observed that the final result is given by contributions of joint points and timelike or spacelike boundaries. Removing the most divergent term by setting  $\tilde{L} = L$ , the corresponding joint contribution,  $\mathcal{J}$ , and timelike and spacelike surface contributions,  $\mathcal{S}_t$ , and  $\mathcal{S}_s$  are given by

$$\mathcal{J} = \frac{V_d L^d}{8\pi G_N} \frac{\log |f(r)|}{r^d}, \quad \mathcal{S}_t = \frac{V_d L^d}{8\pi G_N} \frac{\tilde{\tau}}{2r_h^{d+1}}, \quad \mathcal{S}_s = \frac{V_d L^d}{8\pi G_N} \frac{(d-1)\tau}{2r_h^{d+1}}. \quad (4.1)$$

Note that when the joint point occurs at the horizon one needs to take  $r \rightarrow r_h$  limit from the above joint contribution  $\mathcal{J}$  that typically results to an expression proportional to  $\log |uv| + c_0$ .

Clearly when the joint point is located at the horizon one needs to regularize the joint contribution using equation (2.25). The sign of the joint contribution depends on the position of the corresponding joint point. If the joint point locates on the left or right of the given subregion, the sign is positive and for those that located up or down of the subregion, it is negative. It is also interesting to compute time derivative of the above expressions

$$\dot{\mathcal{J}} = \frac{V_d L^d}{8\pi G_N} \left( \frac{d+1}{2r_h^{d+1}} + \frac{d}{2r^d} f(r) \log |f(r)| \right), \quad \dot{\mathcal{S}}_t = 0, \quad \dot{\mathcal{S}}_s = \frac{V_d L^d}{8\pi G_N} \frac{(d-1)}{2r_h^{d+1}}, \quad (4.2)$$

showing that in the late time the joint point has nontrivial contribution.

Another observation we have made is that whenever the subregion contains a part of black hole interior the finite part of the action is positive and time dependent, while for the cases that the

desired subregion is entirely in the exterior part of the black hole the corresponding finite term is time independent and negative. It is also important to note that for all cases, except one, the most divergent term exhibits volume law scaling with positive sign. These points should be taken into account when it comes to interpret the results from field theory point of view.

Throughout this paper we have been careful enough to clarify what we mean by on-shell action. Indeed there are several terms one may add to action that could alter the results once we compute the on-shell action. It is then important to fix them. Our physical constraints were to have reparametrization invariance and a well-defined variational principle. These assumptions enforce us to have certain boundary and joint actions. In particular it was crucial to consider the log term given by equation (1.2) that is needed to remove the ambiguity associated with the null vectors. Actually in our computations this term has played an essential role.

We note, however, that even with this term the resultant on-shell action still contains an arbitrary length scale. We have chosen the length scale so that the most divergent term of the on-shell action is positive. This is indeed required if one wants to identify the on-shell action with complexity, at least when evaluated inside the WDW patch. Of course following the general idea of the holographic renormalization one may add certain counterterms to remove all divergent terms including that associated with the undetermined length scale [45]. This is, actually, what we have done in this paper when we were only interested in the finite part of the on-shell action.

In fact if one wants to identify the on-shell action with the complexity we may not be surprised to have an arbitrary length scale. This might be related to choosing an arbitrary length scale in the definition of complexity in quantum field theory (see *e.g.* [22, 23]). Of course eventually we would like to find a way to fix the length scale or at least to make a constraint on it so that it could naturally lead to a clear interpretation in terms of complexity.

The main question remains to be addressed is how to interpret our results from field theory point of view. It is well accepted that the on-shell action evaluated in the WDW patch is associated with the computational complexity that is the minimum number of gates one needs to reach the desired target state from reference state (usually the vacuum state). Of course this is the complexity defined for a pure state. It is then natural to look for a definition of complexity for mixed state. This has been partially addressed in [48, 52].

When we are restricted to a subregion, even the whole system is in a pure state, we would have a mixed state density matrix and therefore a definition of mixed state complexity is required. Of course the resultant subregion complexity could as well depend on the state of whole system whether or not it is pure.

Actually different possible definitions of subregion complexity have been explored in [48]. Based on results we have found it seems that the on-shell action evaluated on a subregion in the exterior is better match with purification complexity that is the pure state complexity of a purified state minimizing over all possible purifications. The main observation supporting this proposal is the subadditivity condition satisfied by the corresponding on-shell actions<sup>14</sup>. Note that this is not the

---

<sup>14</sup>We would like to thank B. Swingle for discussions on this point.

case for complexity obtained by CV proposal.

Since we have been dealing with complexity for subregions, motivated by entanglement entropy and mutual information it might be useful to define a new quantity associated with two subregions  $A$  and  $B$  as follows

$$\mathcal{C}(A|B) = \mathcal{C}(A) + \mathcal{C}(B) - \mathcal{C}(A \cup B), \quad (4.3)$$

that could be thought of as mutual complexity. Here  $\mathcal{C}$  stands for complexity evaluated using CA proposal. It also clear that the above expression that it is finite and symmetric under the exchange of subregions  $A$  and  $B$ .

This quantity might be thought of as a quantum measure that measures the correlation between two subsystems. Of course we should admit that the precise interpretation of this quantity is not clear to us. Nonetheless it might be possible to explore certain properties of the quantity. In particular it is interesting to determine the sign of the mutual complexity which in turns could tell us whether the complexity is superadditive or subadditive.

Actually with the context we have been studying the complexity in this paper, it is clear that if one considers two subregions from two different boundaries of the eternal black brane (one from left and the other from right boundaries) the above quantity is negative. More precisely in this case the mutual complexity is given in terms of the on shell action evaluated in the past and future interiors multiplied by a minus sign (see, for example, subsection 2.3.2). Of course, note that in this case since we have to consider all regions inside the horizon, the final results are time dependent.

On the other hand if we are interested in the time independent complexity, we will have to consider cases where both regions are located at the same boundary of the eternal black brane as shown in the Penrose diagram in figure 5. In these cases, being time independent, we will consider a time slice at  $\tau = 0$ . To explore the possible sign of the mutual complexity we first note that in general there is an arbitrary length scale, i.e.  $\tilde{L}$ , in the expression of the complexity that could change the sign as one chooses different scales. This scale appears due to the ambiguity of the normalization of the null vectors (see equation (1.2)).

In fact in subsection 3.2 we have shown that under the assumption of  $\tilde{L} = L$  the subregion complexity is subadditive that means the mutual complexity is positive. This is also consistent with the numerical result found in [52]. It is, however, important to note that a priori there is no reason to fix the new scale  $\tilde{L}$  equal to  $L$  that is AdS radius.

Actually it is straightforward to see that the sign of the mutual complexity defined above also depends on the ratio  $\frac{\tilde{L}}{L}$ . More precisely from equation (3.15) one observes that there are terms proportional to  $\log \frac{\tilde{L}^2}{L^2}$  which could contribute to the mutual complexity whose value is negative for  $\frac{\tilde{L}}{L} > 1$ , Thus this makes the mutual complexity negative. On the other hand for  $\frac{\tilde{L}}{L} \leq 1$ , their contributions are positive that in turns make the mutual complexity positive too.

To conclude we note that the mutual complexity is positive for the cases where the subregion complexity is time independent and moreover  $\frac{\tilde{L}}{L} \leq 1$ . It would be interesting to further explore properties of the mutual complexity which could be though of a quantity that diagnoses whether the complexity is sub or super additive.

## Acknowledgements

The authors would like to kindly thank A. Akhavan, J. L. F. Barbon, A. Naseh, F. Omidi, B. Swingle, M. R. Tanhayi and M.H. Vahidinia for useful comments and discussions on related topics. We would also like to thank the referee for his/her useful comment.

## References

- [1] L. Susskind, “Computational Complexity and Black Hole Horizons,” *Fortsch. Phys.* **64**, 24 (2016) doi:10.1002/prop.201500092 [[arXiv:1403.5695](#) [hep-th], [arXiv:1402.5674](#) [hep-th]].
- [2] D. Stanford and L. Susskind, “Complexity and Shock Wave Geometries,” *Phys. Rev. D* **90**, no. 12, 126007 (2014) doi:10.1103/PhysRevD.90.126007 [[arXiv:1406.2678](#) [hep-th]].
- [3] A. R. Brown, D. A. Roberts, L. Susskind, B. Swingle and Y. Zhao, “Holographic Complexity Equals Bulk Action?,” *Phys. Rev. Lett.* **116**, no. 19, 191301 (2016) doi:10.1103/PhysRevLett.116.191301 [[arXiv:1509.07876](#) [hep-th]].
- [4] A. R. Brown, D. A. Roberts, L. Susskind, B. Swingle and Y. Zhao, “Complexity, action, and black holes,” *Phys. Rev. D* **93**, no. 8, 086006 (2016) doi:10.1103/PhysRevD.93.086006 [[arXiv:1512.04993](#) [hep-th]].
- [5] M. Alishahiha, “Holographic Complexity,” *Phys. Rev. D* **92**, no. 12, 126009 (2015) doi:10.1103/PhysRevD.92.126009 [[arXiv:1509.06614](#) [hep-th]].
- [6] O. Ben-Ami and D. Carmi, “On Volumes of Subregions in Holography and Complexity,” *JHEP* **1611**, 129 (2016) doi:10.1007/JHEP11(2016)129 [[arXiv:1609.02514](#) [hep-th]].
- [7] J. Couch, W. Fischler and P. H. Nguyen, “Noether charge, black hole volume and complexity,” [arXiv:1610.02038](#) [hep-th].
- [8] D. Carmi, R. C. Myers and P. Rath, “Comments on Holographic Complexity,” [arXiv:1612.00433](#) [hep-th].
- [9] R. Abt, J. Erdmenger, H. Hinrichsen, C. M. Melby-Thompson, R. Meyer, C. Northe and I. A. Reyes, “Topological Complexity in  $\text{AdS}_3/\text{CFT}_2$ ,” *Fortsch. Phys.* **66**, no. 6, 1800034 (2018) doi:10.1002/prop.201800034 [[arXiv:1710.01327](#) [hep-th]].
- [10] R. Abt, J. Erdmenger, M. Gerbershagen, C. M. Melby-Thompson and C. Northe, “Holographic Subregion Complexity from Kinematic Space,” [arXiv:1805.10298](#) [hep-th].
- [11] E. Bakhshaei, A. Mollabashi and A. Shirzad, “Holographic Subregion Complexity for Singular Surfaces,” *Eur. Phys. J. C* **77**, no. 10, 665 (2017) doi:10.1140/epjc/s10052-017-5247-1 [[arXiv:1703.03469](#) [hep-th]].



- [12] B. Chen, W. M. Li, R. Q. Yang, C. Y. Zhang and S. J. Zhang, “Holographic subregion complexity under a thermal quench,” JHEP **1807**, 034 (2018) doi:10.1007/JHEP07(2018)034 [[arXiv:1803.06680](#) [hep-th]].
- [13] D. S. Ageev, I. Y. Aref’eva, A. A. Bagrov and M. I. Katsnelson, “Holographic local quench and effective complexity,” JHEP **1808**, 071 (2018) doi:10.1007/JHEP08(2018)071 [[arXiv:1803.11162](#) [hep-th]].
- [14] M. Miyaji, T. Takayanagi and K. Watanabe, “From path integrals to tensor networks for the AdS/CFT correspondence,” Phys. Rev. D **95**, no. 6, 066004 (2017) doi:10.1103/PhysRevD.95.066004 [[arXiv:1609.04645](#) [hep-th]].
- [15] P. Caputa, N. Kundu, M. Miyaji, T. Takayanagi and K. Watanabe, “Anti-de Sitter Space from Optimization of Path Integrals in Conformal Field Theories,” Phys. Rev. Lett. **119**, no. 7, 071602 (2017) doi:10.1103/PhysRevLett.119.071602 [[arXiv:1703.00456](#) [hep-th]].
- [16] P. Caputa, N. Kundu, M. Miyaji, T. Takayanagi and K. Watanabe, “Liouville Action as Path-Integral Complexity: From Continuous Tensor Networks to AdS/CFT,” JHEP **1711**, 097 (2017) doi:10.1007/JHEP11(2017)097 [[arXiv:1706.07056](#) [hep-th]].
- [17] T. Takayanagi, “Holographic Spacetimes as Quantum Circuits of Path-Integrations,” [arXiv:1808.09072](#) [hep-th].
- [18] D. Carmi, S. Chapman, H. Marrochio, R. C. Myers and S. Sugishita, “On the Time Dependence of Holographic Complexity,” JHEP **1711**, 188 (2017) doi:10.1007/JHEP11(2017)188 [[arXiv:1709.10184](#) [hep-th]].
- [19] S. Lloyd, “Ultimate physical limits to computation,” Nature **406** (2000) 1047, [[arXiv:quant-ph/9908043](#)].
- [20] M. Moosa, “Evolution of Complexity Following a Global Quench,” [arXiv:1711.02668](#) [hep-th].
- [21] K. Hashimoto, N. Iizuka and S. Sugishita, “Time evolution of complexity in Abelian gauge theories,” Phys. Rev. D **96**, no. 12, 126001 (2017) doi:10.1103/PhysRevD.96.126001 [[arXiv:1707.03840](#) [hep-th]].
- [22] R. Jefferson and R. C. Myers, “Circuit complexity in quantum field theory,” JHEP **1710**, 107 (2017) doi:10.1007/JHEP10(2017)107 [[arXiv:1707.08570](#) [hep-th]].
- [23] S. Chapman, M. P. Heller, H. Marrochio and F. Pastawski, “Toward a Definition of Complexity for Quantum Field Theory States,” Phys. Rev. Lett. **120**, no. 12, 121602 (2018) doi:10.1103/PhysRevLett.120.121602 [[arXiv:1707.08582](#) [hep-th]].
- [24] R. Q. Yang, “Complexity for quantum field theory states and applications to thermofield double states,” Phys. Rev. D **97**, no. 6, 066004 (2018) doi:10.1103/PhysRevD.97.066004 [[arXiv:1709.00921](#) [hep-th]].

- [25] R. Khan, C. Krishnan and S. Sharma, “Circuit Complexity in Fermionic Field Theory,” [arXiv:1801.07620](#) [hep-th].
- [26] R. Q. Yang, Y. S. An, C. Niu, C. Y. Zhang and K. Y. Kim, “Principles and symmetries of complexity in quantum field theory,” *Eur. Phys. J. C* **79**, no. 2, 109 (2019) doi:10.1140/epjc/s10052-019-6600-3 [[arXiv:1803.01797](#) [hep-th]].
- [27] L. Hackl and R. C. Myers, “Circuit complexity for free fermions,” *JHEP* **1807**, 139 (2018) [*Physics* **2018**, 139 (2018)] doi:10.1007/JHEP07(2018)139 [[arXiv:1803.10638](#) [hep-th]].
- [28] D. W. F. Alves and G. Camilo, “Evolution of complexity following a quantum quench in free field theory,” *JHEP* **1806**, 029 (2018) doi:10.1007/JHEP06(2018)029 [[arXiv:1804.00107](#) [hep-th]].
- [29] A. Bhattacharyya, P. Caputa, S. R. Das, N. Kundu, M. Miyaji and T. Takayanagi, “Path-Integral Complexity for Perturbed CFTs,” *JHEP* **1807**, 086 (2018) doi:10.1007/JHEP07(2018)086 [[arXiv:1804.01999](#) [hep-th]].
- [30] M. Guo, J. Hernandez, R. C. Myers and S. M. Ruan, “Circuit Complexity for Coherent States,” [arXiv:1807.07677](#) [hep-th].
- [31] A. Bhattacharyya, A. Shekar and A. Sinha, “Circuit complexity in interacting QFTs and RG flows,” [arXiv:1808.03105](#) [hep-th].
- [32] R. Q. Yang, Y. S. An, C. Niu, C. Y. Zhang and K. Y. Kim, “More on complexity of operators in quantum field theory,” [arXiv:1809.06678](#) [hep-th].
- [33] R. Q. Yang, C. Niu, C. Y. Zhang and K. Y. Kim, “Comparison of holographic and field theoretic complexities for time dependent thermofield double states,” *JHEP* **1802**, 082 (2018) doi:10.1007/JHEP02(2018)082 [[arXiv:1710.00600](#) [hep-th]].
- [34] M. Moosa, “Divergences in the rate of complexification,” *Phys. Rev. D* **97**, no. 10, 106016 (2018) doi:10.1103/PhysRevD.97.106016 [[arXiv:1712.07137](#) [hep-th]].
- [35] B. Swingle and Y. Wang, “Holographic Complexity of Einstein-Maxwell-Dilaton Gravity,” [arXiv:1712.09826](#) [hep-th].
- [36] J. W. York, Jr., “Role of conformal three geometry in the dynamics of gravitation,” *Phys. Rev. Lett.* **28**, 1082 (1972). doi:10.1103/PhysRevLett.28.1082
- [37] G. W. Gibbons and S. W. Hawking, “Action Integrals and Partition Functions in Quantum Gravity,” *Phys. Rev. D* **15**, 2752 (1977). doi:10.1103/PhysRevD.15.2752
- [38] K. Parattu, S. Chakraborty, B. R. Majhi and T. Padmanabhan, “A Boundary Term for the Gravitational Action with Null Boundaries,” *Gen. Rel. Grav.* **48**, no. 7, 94 (2016) doi:10.1007/s10714-016-2093-7 [[arXiv:1501.01053](#) [gr-qc]].

- [39] L. Lehner, R. C. Myers, E. Poisson and R. D. Sorkin, “Gravitational action with null boundaries,” *Phys. Rev. D* **94** (2016) no.8, 084046 doi:10.1103/PhysRevD.94.084046 [[arXiv:1609.00207](#) [hep-th]].
- [40] A. Reynolds and S. F. Ross, “Divergences in Holographic Complexity,” *Class. Quant. Grav.* **34**, no. 10, 105004 (2017) doi:10.1088/1361-6382/aa6925 [[arXiv:1612.05439](#) [hep-th]].
- [41] M. Alishahiha, A. Faraji Astaneh, M. R. Mohammadi Mozaffar and A. Mollabashi, “Complexity Growth with Lifshitz Scaling and Hyperscaling Violation,” *JHEP* **1807**, 042 (2018) doi:10.1007/JHEP07(2018)042 [[arXiv:1802.06740](#) [hep-th]].
- [42] S. Chapman, H. Marrochio and R. C. Myers, “Holographic complexity in Vaidya spacetimes. Part I,” *JHEP* **1806**, 046 (2018) doi:10.1007/JHEP06(2018)046 [[arXiv:1804.07410](#) [hep-th]].
- [43] S. Chapman, H. Marrochio and R. C. Myers, “Holographic complexity in Vaidya spacetimes. Part II,” *JHEP* **1806**, 114 (2018) doi:10.1007/JHEP06(2018)114 [[arXiv:1805.07262](#) [hep-th]].
- [44] K. Skenderis, “Lecture notes on holographic renormalization,” *Class. Quant. Grav.* **19**, 5849 (2002) doi:10.1088/0264-9381/19/22/306 [[hep-th/0209067](#)].
- [45] A. Akhavan and F. Omid, “Complexity and the Role of Counter Terms,” To appear.
- [46] S. Chapman, H. Marrochio and R. C. Myers, “Complexity of Formation in Holography,” *JHEP* **1701**, 062 (2017) doi:10.1007/JHEP01(2017)062 [[arXiv:1610.08063](#) [hep-th]].
- [47] J. L. F. Barbon and J. Martin-Garcia, “Terminal Holographic Complexity,” *JHEP* **1806**, 132 (2018) doi:10.1007/JHEP06(2018)132 [[arXiv:1805.05291](#) [hep-th]].
- [48] C. A. Agon, M. Headrick and B. Swingle, “Subsystem Complexity and Holography,” [arXiv:1804.01561](#) [hep-th].
- [49] A. R. Brown and L. Susskind, “Second law of quantum complexity,” *Phys. Rev. D* **97**, no. 8, 086015 (2018) doi:10.1103/PhysRevD.97.086015 [[arXiv:1701.01107](#) [hep-th]].
- [50] Y. Zhao, “Uncomplexity and Black Hole Geometry,” *Phys. Rev. D* **97**, no. 12, 126007 (2018) doi:10.1103/PhysRevD.97.126007 [[arXiv:1711.03125](#) [hep-th]].
- [51] H. Stoltenberg, “Properties of the (Un)Complexity of Subsystems,” [arXiv:1807.05218](#) [quant-ph].
- [52] H. A. Camargo, P. Caputa, D. Das, M. P. Heller and R. Jefferson, “Complexity as a novel probe of quantum quenches: universal scalings and purifications,” [arXiv:1807.07075](#) [hep-th].
- [53] D. Momeni, M. Faizal, S. Bahamonde and R. Myrzakulov, “Holographic complexity for time-dependent backgrounds,” *Phys. Lett. B* **762**, 276 (2016) doi:10.1016/j.physletb.2016.09.036 [[arXiv:1610.01542](#) [hep-th]].

- [54] M. Alishahiha, A. Faraji Astaneh, A. Naseh and M. H. Vahidinia, “On complexity for  $F(R)$  and critical gravity,” JHEP **1705**, 009 (2017) doi:10.1007/JHEP05(2017)009 [[arXiv:1702.06796](#) [hep-th]].
- [55] K. Nagasaki, “Complexity of  $AdS_5$  black holes with a rotating string,” Phys. Rev. D **96**, no. 12, 126018 (2017) doi:10.1103/PhysRevD.96.126018 [[arXiv:1707.08376](#) [hep-th]].
- [56] Y. G. Miao and L. Zhao, “Complexity-action duality of the shock wave geometry in a massive gravity theory,” Phys. Rev. D **97**, no. 2, 024035 (2018) doi:10.1103/PhysRevD.97.024035 [[arXiv:1708.01779](#) [hep-th]].
- [57] M. Ghodrati, “Complexity growth in massive gravity theories, the effects of chirality, and more,” Phys. Rev. D **96**, no. 10, 106020 (2017) doi:10.1103/PhysRevD.96.106020 [[arXiv:1708.07981](#) [hep-th]].
- [58] M. M. Qaemmaqami, “Complexity growth in minimal massive 3D gravity,” Phys. Rev. D **97**, no. 2, 026006 (2018) doi:10.1103/PhysRevD.97.026006 [[arXiv:1709.05894](#) [hep-th]].
- [59] L. Sebastiani, L. Vanzo and S. Zerbini, “Action growth for black holes in modified gravity,” Phys. Rev. D **97**, no. 4, 044009 (2018) doi:10.1103/PhysRevD.97.044009 [[arXiv:1710.05686](#) [hep-th]].
- [60] P. A. Cano, R. A. Hennigar and H. Marrochio, “Complexity Growth Rate in Lovelock Gravity,” [arXiv:1803.02795](#) [hep-th].
- [61] Y. S. An, R. G. Cai and Y. Peng, “Time Dependence of Holographic Complexity in Gauss-Bonnet Gravity,” [arXiv:1805.07775](#) [hep-th].
- [62] R. Fareghbal and P. Karimi, “Complexity growth in flat spacetimes,” Phys. Rev. D **98**, no. 4, 046003 (2018) doi:10.1103/PhysRevD.98.046003 [[arXiv:1806.07273](#) [hep-th]].
- [63] M. Ghodrati, “Complexity growth rate during phase transitions,” [arXiv:1808.08164](#) [hep-th].
- [64] S. J. Zhang, “Subregion complexity and confinement-deconfinement transition in a holographic QCD model,” [arXiv:1808.08719](#) [hep-th].
- [65] S. Mahapatra and P. Roy, “On the time dependence of holographic complexity in a dynamical Einstein-dilaton model,” [arXiv:1808.09917](#) [hep-th].
- [66] M. R. Tanhayi, R. Vazirian and S. Khoeini-Moghaddam, “Complexity Growth Following Multiple Shocks,” [arXiv:1809.05044](#) [hep-th].